

Name: Andrés Felipe Jerez Ariza Scholar ID: 2188136

1 Introduction

In standard big bang cosmology theory [Freedman et al.2001], the Universe expands uniformly and locally according to the Hubble law is given by

$$v = H_0 \times d, \quad (1)$$

where v is the recesssion speed of a galaxy at a distance d and H_0 is the Hubble constant, which corresponds to the expansion rate at the current epoch. Specifically, the hubble constant enters in a practical way into numerous cosmological and astrophysical calculations. The Hubble constant inverse H_0^{-1} sets the age of the Universe t_0 .

However, the distance and speed of a galaxy cannot be directly measured. Traditionally, the distance to a galaxy is estimated by measuring the apparent brightness of an object (I_{obs}) whose intrinsic brightness (I_0) is known. Hence, this the diminution of brightness allows calculating the distance to the galaxy in which it lives. This physical quantity is called luminous distance D_L

$$I_{obs} = \frac{1}{4\pi D_L^2}, \quad (2)$$

Generally, the brightness of astronomical objects is usually measured on a logarithmic scale as

$$\mu = 5 \log_{10}(D_L) + 25 \quad (3)$$

In addition, the velocity is measured by a change of frequency of the emitted light for the galaxy due to the Doppler effect. If a galaxy moves away, the waves of light that reach us will have longer wavelengths, that is, frequencies smaller than those that are actually being emitted by the source. Then, the light emitted by the objects that move away presents a redder color to its real color, besides, when measuring the fractional change in the wavelength, commonly known as redshift (z), it can be inferred the speed that a source is moved away compared to the speed of light (c)

$$z = \frac{\lambda_{obs} - \lambda_{em}}{\lambda_{em}} = \frac{v}{c}, \quad (4)$$

where λ_{obs} and λ_{em} correspond to the observed light and measured light, respectively.

Notice that the redshift observed in the light of a galaxy indicates the size of the Universe at the moment when the galaxy emitted its light compared to the size of the Universe today. The luminous distance according to each redshift and considering the amount of matter and energy that exists in

the Universe is mathematically defined as

$$D_L(z) = \begin{cases} \frac{(1+z)}{H_0} \frac{1}{\sqrt{|\Omega_K|}} \sin\left(\sqrt{|\Omega_K|}I\right) & , \text{if } \Omega_M + \Omega_\Lambda > 1 \\ \frac{(1+z)}{H_0} I & , \text{if } \Omega_M + \Omega_\Lambda = 1, \\ \frac{(1+z)}{H_0} \frac{1}{\sqrt{|\Omega_K|}} \sinh\left(\sqrt{|\Omega_K|}I\right) & , \text{if } \Omega_M + \Omega_\Lambda < 1 \end{cases} \quad (5)$$

where Ω_M represents the percentage of the Universe that is composed of matter, Ω_Λ is the percentage of the energy of the Universe in the shape of dark energy and Ω_K corresponds to the curvature of the Universe. If Ω_K is equal to zero it refers to a flat Universe, and if Ω_K is greater or lesser than zero it corresponds to opened and closed Universe models, respectively. These quantities are related by $\Omega_M + \Omega_\Lambda + \Omega_K = 1$. Additionally, I is denoted by

$$I = \int_0^z \frac{1}{\sqrt{\Omega_M(1+z)^3 + \Omega_\Lambda + \Omega_K(1+z)^2}} \quad (6)$$

This work presents several simulation results in order to study the Universe expansion from the Hubble law and type IA supernovae, which allows analyzing the behavior of cosmological parameters Ω_M , Ω_Λ and Ω_K .

2 Simulation Results

In this section, the simulation results about Hubble law and the calculus of cosmological parameters that describe the Universe are presented. Specifically, four datasets (1929, 1936, Recent, supernovae) are employed in order to study some cosmological properties, dataset 1929, 1936 and recent correspond to distance and speed data about some objects measured in those epochs for studying the Hubble law. The dataset about supernovae was extracted on <http://supernova.lbl.gov/Union/>, which contains redshift, distance, and error of the distance about some objects for analyzing the Universe models.

2.1 Hubble Constant Analysis

In Fig. 1 the adjustment and original dataset that contain the distance and speed of some objects are shown. Notice that in 1929 the farthest object that could be measured was around $2[Mpc]$, due to the technological limitations of the epoch. Then, thanks to technological advances, it was possible to obtain measurements of more distant objects of up to $80[Mpc]$.

Table 1 shows the estimated Hubble constants through the adjustment at each dataset as Fig. 1, for instance, the approximations evaluated by using datasets measured in 1929, 1936 and combinations of these datasets present the worst estimations, due to the Universe time calculated through these Hubble constants does not achieve the age of some globular agglomerates that correspond to $9000[myr]$. Therefore, the Hubble constants estimated in 1929 and 1936 does not allow correctly describing the behavior of the Universe in those epochs. Further, the recent experiments could present a better approximation to Hubble constant, due to the estimated Universe time is greater than some globular agglomerates. Also, these behaviors are directly related to the distance of objects measured at each epoch, i.e., as it is possible to measure more distant objects, a better estimation of the Hubble constant. The value of the most accepted Hubble constant equals to $68[\frac{km}{s} \frac{1}{Mpc}]$, which compared to the recent dataset is a good approximation, the Hubble constant estimate with the 1929, 1936 datasets and the combined datasets present the worst approximation.

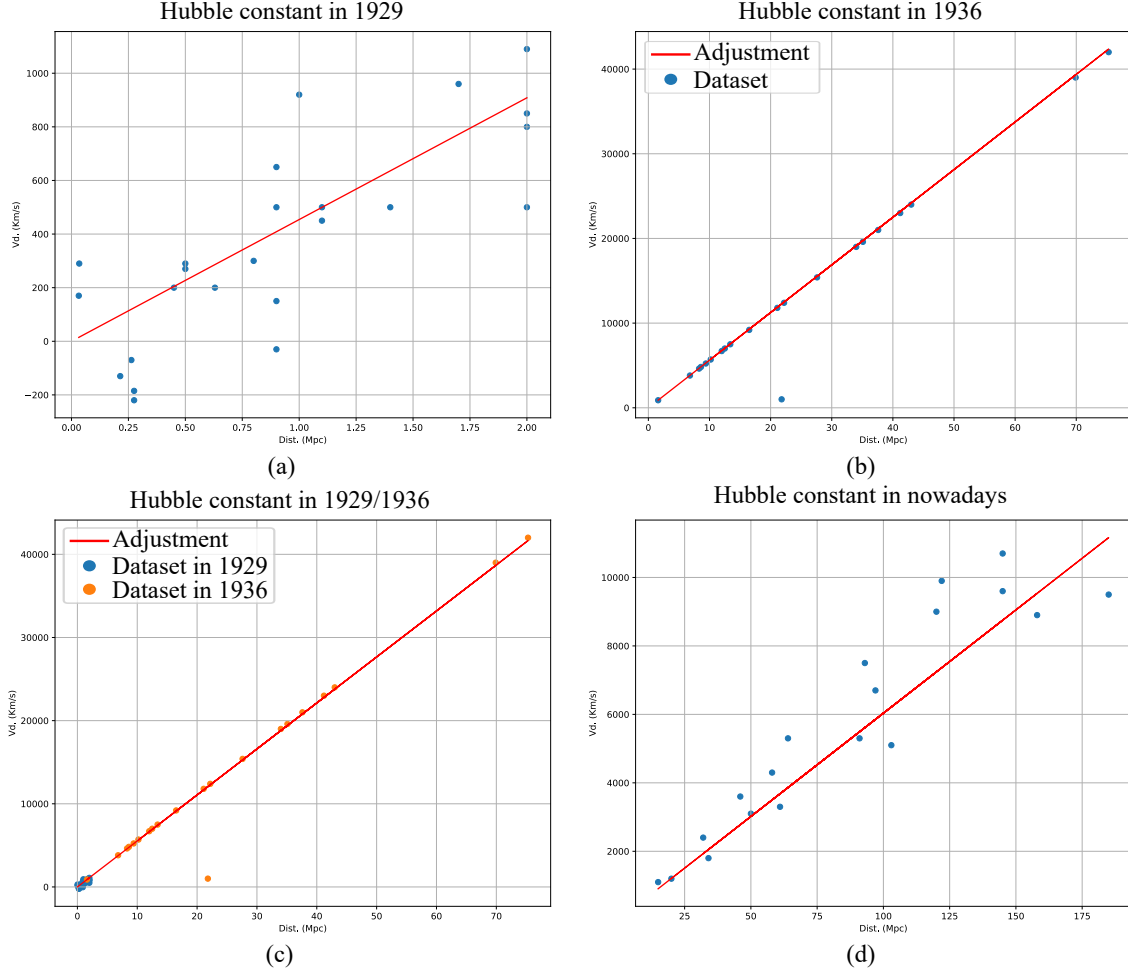


Figure 1: Hubble constant analysis by using datasets collected in (a) 1929, (b) 1936, (c) 1929/1936 and (d) some recent experiments.

Dataset	Estimated Hubble constant $\left[\frac{km/s}{Mpc}\right]$	Estimated time $[myr]$
1929	454.158	2154.402
1936	562.545	1739.311
1929/1936	553.156	1768.833
Recent	60.345	16213.97

Table 1: Hubble constant calculated through different datasets and estimated time according to each approximated Hubble constant. Here, *myr* represents the abbreviation of million years.

2.2 Supernovae Analysis

Fig. 2 shows the theoretical models expected using different setup of the cosmological parameters and the data with and the data with their respective error bars. Specifically, three theoretical models were described: the first model represents a Universe without dark energy ($\Omega_M = 0.3$), the second model shows a Universe with excess dark energy ($\Omega_M = 0.3, \Omega_\Lambda = 1.0$), and the third model describes a standard Universe ($\Omega_M = 0.28, \Omega_\Lambda = 0.72$). In addition, Fig. 3 illustrates the observed Hubble law according to the distribution of supernovae, particularly, nearby supernovae around

redshift lower than 0.0356 retain a behavior as described by Hubble Law unlike distant supernovae, where this law is not completely fulfilled.

In Fig. 4 presents the best adjustment of the theoretical model using combinations of the cosmological parameters calculated by a minimization of the quadratic error. More precisely, the obtained cosmological parameters through the minimization algorithm are ($\Omega_M = 0.121968, \Omega_\Lambda = 0.369806, \Omega_K = 0.508226$).

On the other hand, Fig. 5 illustrates the calculated cosmological parameters through a Monte-Carlo chain considering three different initial points (Ω_M, Ω_Λ): point 1 ($\Omega_M = 0.261768, \Omega_\Lambda = 0.611828$), point 3 ($\Omega_M = 0.115438, \Omega_\Lambda = 0.309058$) and point 1 ($\Omega_M = 0.115496, \Omega_\Lambda = 0.378609$). The best obtained cosmological parameters using Monte-Carlo chain was ($\Omega_M = 0.141179, \Omega_\Lambda = 0.393481$). Furthermore, Fig. 6 presents the confidence intervals $\in \{68.3\%, 90\%, 95.4\%, 99\%\}$ considering $\Delta_\chi^2 \in \{2.3, 4.61, 6.17, 9.21\}$, respectively. In Fig. 7 the probability function of the marginal probabilities at each cosmological parameter (Ω_M, Ω_Λ) is shown, where the adjustment probability function $P(\Omega_M)$ has a mean of 0.398169 and standard deviation of 0.854554 and the adjustment probability function $P(\Omega_\Lambda)$ has a mean of 0.990367 and standard deviation of 0.798130. Additionally, the confidence intervals and probability function of the marginal probabilities at each cosmological parameter (Ω_M, Ω_Λ) were analyzed taking lower redshifts such as $z < 0.3$. Figs. 8 and 9 presents the confidence intervals and marginal probabilities using lower redshifts with a mean of 4.148084 and standar deviation of 3.409067, respectively. Specifically, the adjustment probability function $P(\Omega_M)$ has a mean of 0.775653 and standard deviation of 3.764604 and the adjustment probability function $P(\Omega_\Lambda)$ has a mean of 1.021755 and standard deviation of 0.978382.

Finally, Table 2 presents the analysis of the Trotta criterion considering the best cosmological parameter (Ω_M, Ω_Λ) obtained using Monte-Carlo chain. Although some perturbations were introduced to this parameter configuration, the criterion seems to be plausible for all cases, due to the behavior of the confidence intervals of these parameters with respect to the quadratic residual χ^2 .

Disturbance	Likelihood	Trotta criterion	Interpretation
-1%	0.606508	0.999963	Strong
-5%	0.606370	0.999736	Strong
-20%	0.606153	0.999378	Strong
+1%	0.606547	1.000028	Strong
+5%	0.606567	1.000060	Strong
+20%	0.606507	0.999961	Strong

Table 2: Comparison models using Trotta criterion.

References

- [Freedman et al.2001] Freedman, W. L., Madore, B. F., Gibson, B. K., Ferrarese, L., Kelson, D. D., Sakai, S., Mould, J. R., Kennicutt Jr, R. C., Ford, H. C., Graham, J. A., et al. (2001). Final results from the hubble space telescope key project to measure the hubble constant. *The Astrophysical Journal*, 553(1):47.

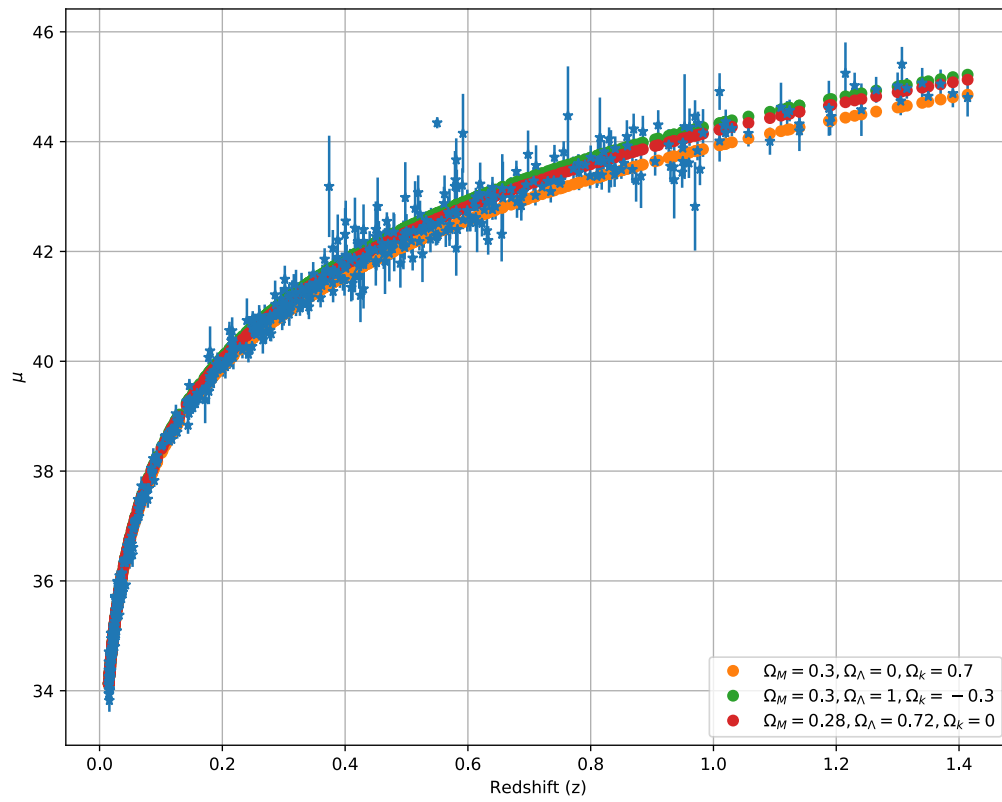


Figure 2: Theoretical models expected by varying the cosmological parameters.

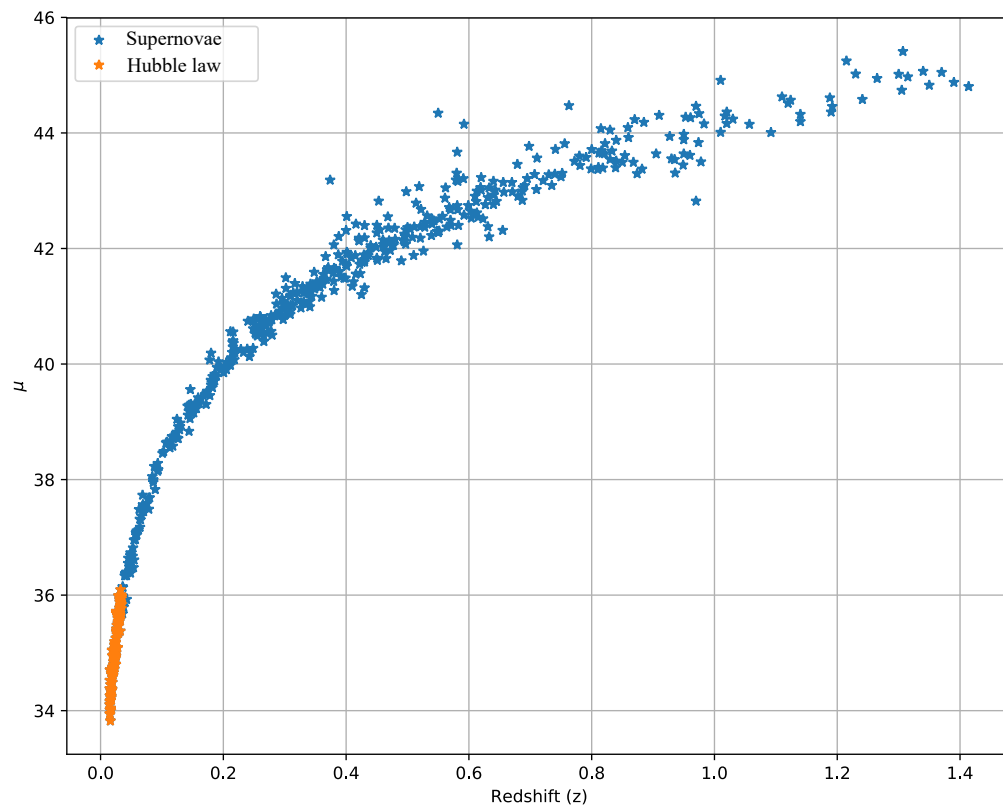


Figure 3: Hubble Law in supernovae.

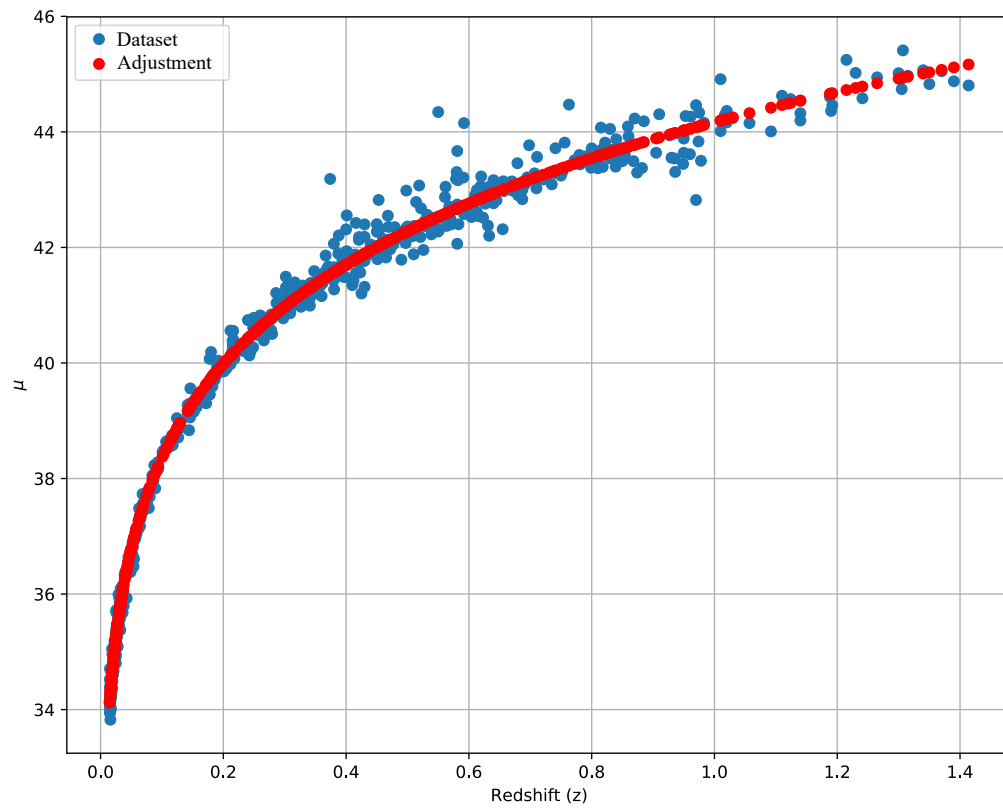


Figure 4: The best-obtained adjustment by minimization of quadratic error in function of the cosmological parameters.

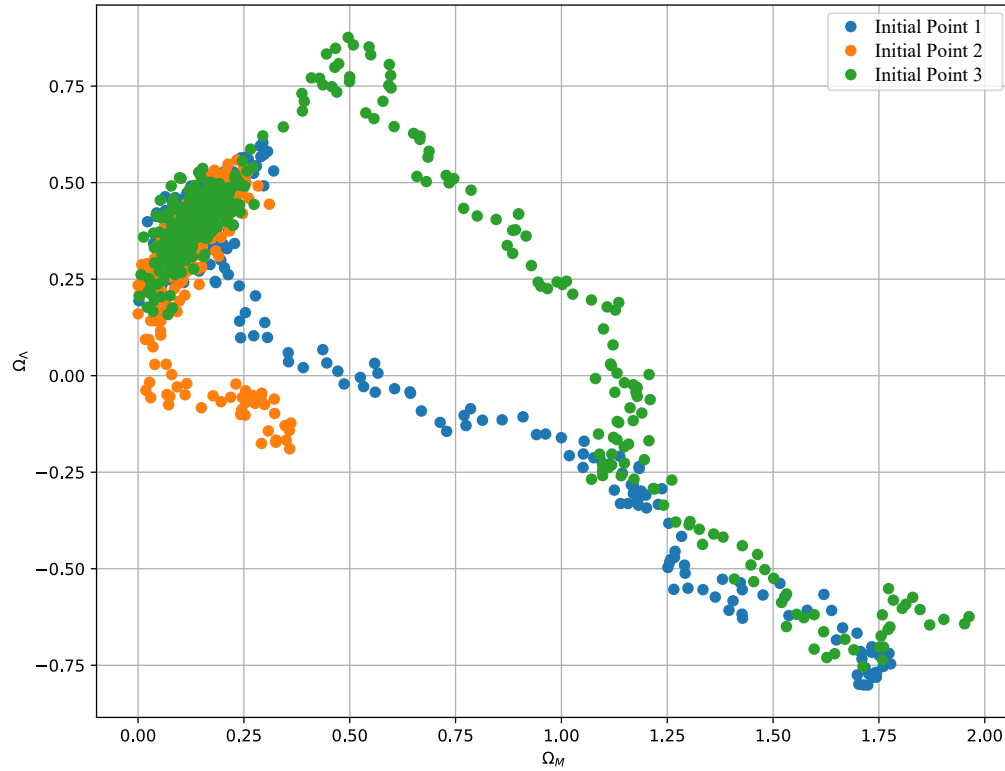


Figure 5: Analysis of cosmological parameters obtained by Monte-Carlo Markov chain.

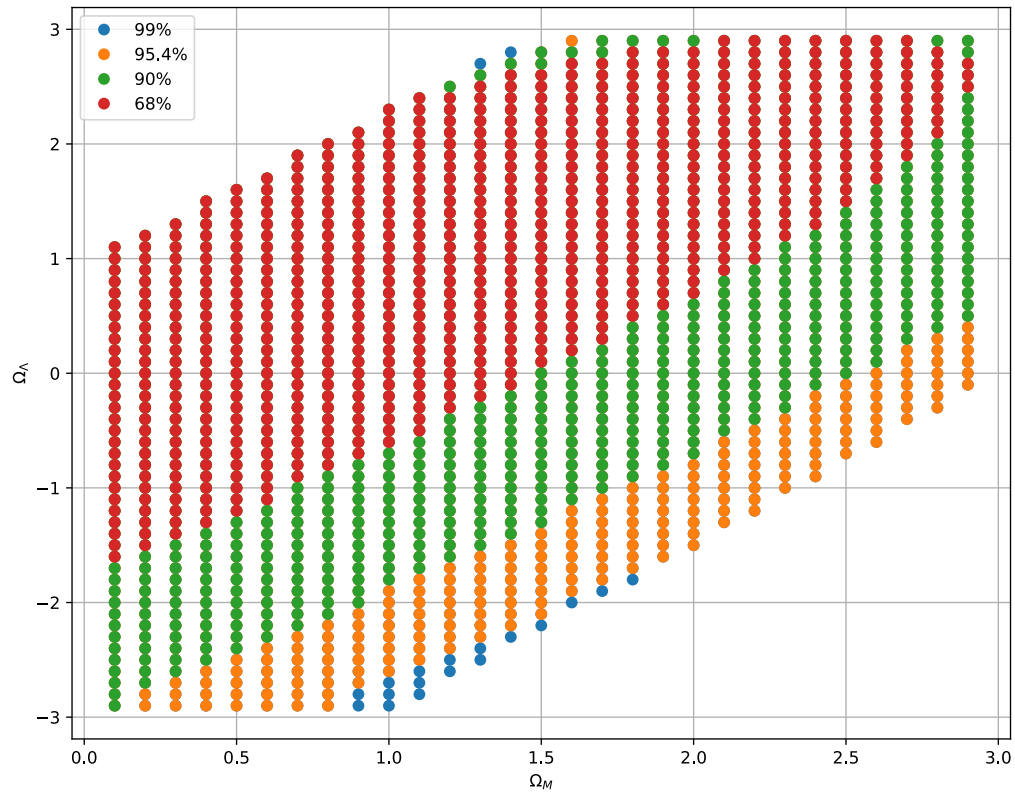


Figure 6: Quadratic residue behavior χ^2 .

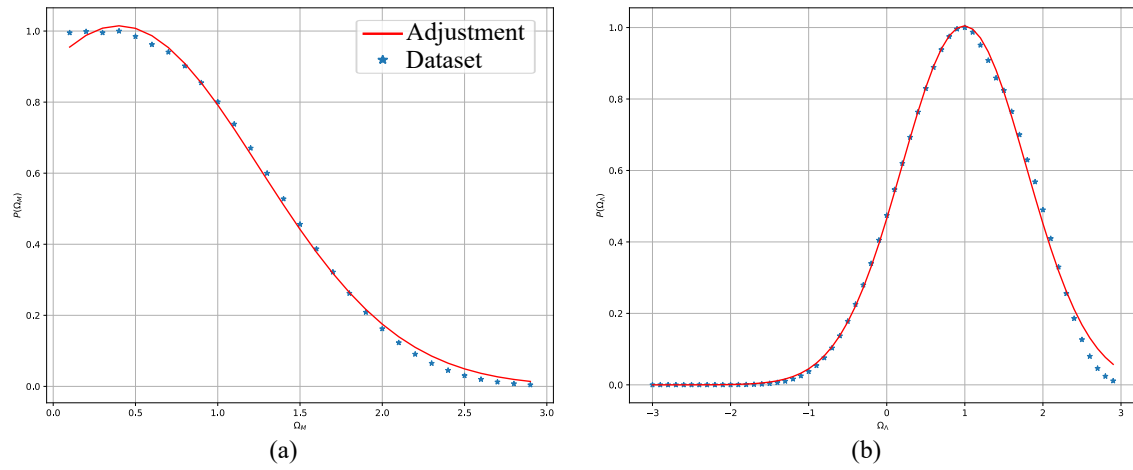


Figure 7: Marginal probabilities. (a) $P(\Omega_M)$. (b) $P(\Omega_\Lambda)$.

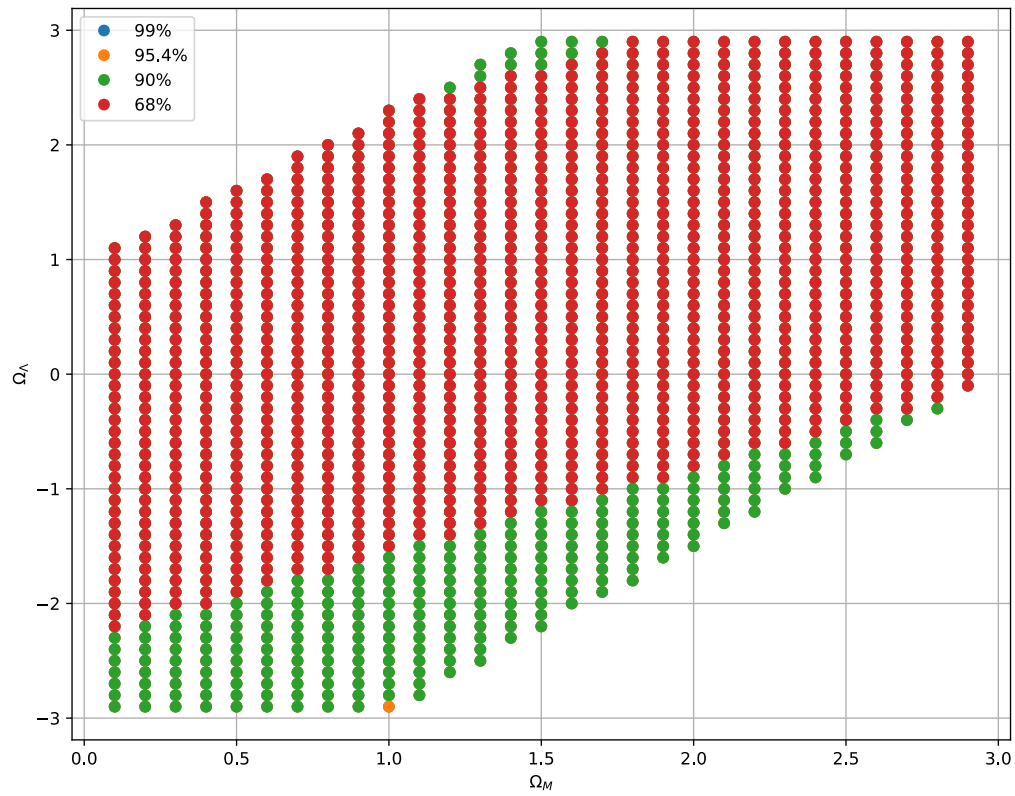


Figure 8: Quadratic residue behavior χ^2 using redshift $z < 0.3$.

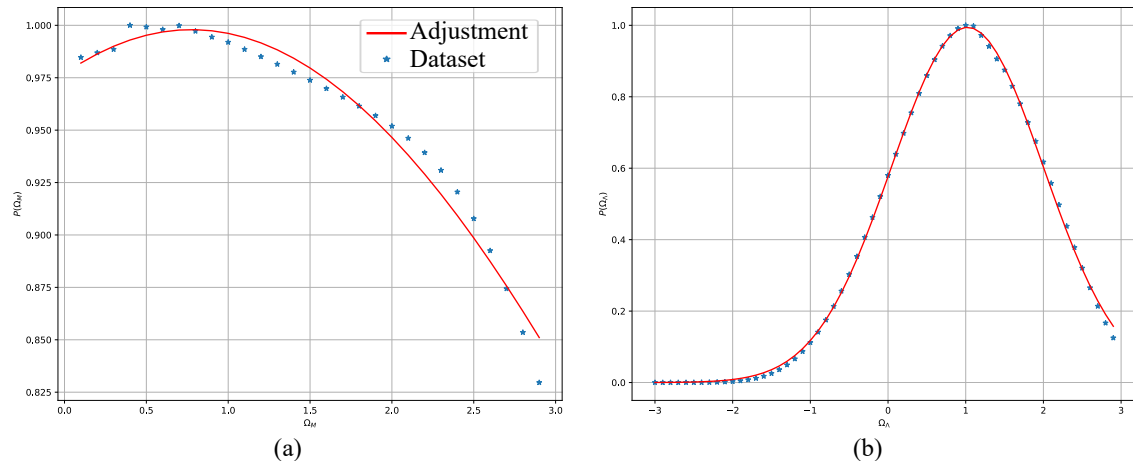


Figure 9: Marginal probabilities using redshift $z < 0.3$. (a) $P(\Omega_M)$. (b) $P(\Omega_\Lambda)$.